Characterization of the Structure and Membrane Interaction of the Antimicrobial Peptides Aurein 2.2 and 2.3 from Australian Southern Bell Frogs

Yeang-Ling Pan,* John T.-J. Cheng,* John Hale,† Jinhe Pan,* Robert E. W. Hancock,† and Suzana K. Straus*
*Department of Chemistry, University of British Columbia, Vancouver, British Columbia, V6T 1Z1, Canada; and †Centre for Microbial Diseases and Immunity Research, University of British Columbia, Vancouver, British Columbia, V6T 1Z3, Canada

ABSTRACT The structure and membrane interaction of the antimicrobial peptide aurein 2.2 (GLFDIVKKVVGALGSL-$CONH_2$), aurein 2.3 (GLFDIVKKVVGAIGSL-$CONH_2$), both from *Litoria aurea*, and a carboxy C-terminal analog of aurein 2.3 (GLFDIVKKVVGAIGSL-COOH) were studied to determine which features of this class of peptides are key to activity. Circular dichroism and solution-state NMR data indicate that all three peptides adopt an α-helical structure in the presence of trifluoroethanol or lipids such as 1,2-dimyristoyl-*sn*-glycero-3-phosphocholine (DMPC) and a 1:1 mixture of DMPC and 1,2-dimyristoyl-*sn*-glycero-3-[phospho-*rac*-(1-glycerol)] (DMPG). Oriented circular dichroism was used to determine the orientation of the peptides in lipid bilayers over a range of concentrations (peptide/lipid molar ratios (P/L) = 1:15–1:120) in DMPC and 1:1 DMPC/DMPG, in the liquid crystalline state. The results demonstrate that in DMPC all three peptides are surface adsorbed over a range of low peptide concentrations but insert into the bilayers at high peptide concentrations. This finding is corroborated by ^{31}P-solid-state NMR data of the three peptides in DMPC, which shows that at high peptide concentrations the peptides perturb the membrane. Oriented circular dichroism data of the aurein peptides in 1:1 DMPC/DMPG, on the other hand, show that the peptides with amidated C-termini readily insert into the membrane bilayers over the concentration range studied (P/L = 1:15–1:120), whereas the aurein 2.3 peptide with a carboxy C-terminus inserts at a threshold concentration of P/L* between 1:80 and 1:120. Overall, the data presented here suggest that all three peptides studied interact with phosphatidylcholine membranes in a manner which is similar to aurein 1.2 and citropin 1.1, as reported in the literature, with no correlation to the reported activity. On the other hand, both aurein 2.2 and aurein 2.3 behave similarly in phosphatidylcholine/phosphatidylglycerol (PC/PG) membranes, whereas aurein 2.3-COOH inserts less readily. As this does not correlate with reported activities, minimal inhibitory concentrations of the three peptides against *Staphylococcus aureus* (strain C622, ATCC 25923) and *Staphylococcus epidermidis* (strain C621—clinical isolate) were determined. The correlation between structure, membrane interaction, and activity are discussed in light of these results.

INTRODUCTION

Cationic antimicrobial peptides are an important class of peptides which target a wide range of microbes, such as bacteria and fungi, and disease-causing agents, such as cancer cells and viruses (1,2). They are ubiquitous in the animal and plant kingdoms and constitute an important part of the immune defense system. To date, they have displayed little or no resistance effects (3–5), making them prime targets for development as a new class of antiinfective agents. The thousand peptides identified to date share a common three-dimensional arrangement in the presence of membranes, despite the diversity in the amino acid sequences and structures (e.g., β-sheets, α-helices, loops, and extended structures) they adopt (1). They form amphiphilic molecules, where one face of the peptide is hydrophobic and the other is positively charged (3), thereby allowing them to interact and bind with the negatively charged bacterial membranes. A model which can be used to account for the initial interactions of most antimicrobial peptides with membranes is the Shai-Matsuzaki-Huang model (6–10). Briefly, this model proposes that the peptides are initially unstructured in solution and fold in the presence of membranes or membrane mimetics. The peptides then integrate into the outer half of the membrane, leading to thinning of the outer leaflet (11–13). This is followed by membrane disruption via a barrel-stave model, carpet model, toroidal pore model, micellar aggregate channel model (14,15), or detergent-like mechanism (16). Finally, the bacterial cells are killed via, for example, membrane depolarization, degradation of cell walls, and micellization, to name a few mechanisms (17).

An important family of cationic antimicrobial peptides is those secreted by amphibians. When these animals are exposed to a variety of stimuli, host-defense compounds, consisting of amines, alkaloids, and peptides, are secreted (18). A great many studies have been performed on peptides obtained from amphibians and have been reviewed extensively in the literature (for recent reviews, see Zasloff (2), Pukala et al. (18), and Rinaldi (19)). Examples of a few amphibian host-defense peptides include magainins (9,20–28), maculatins (29–34), and brevinins (35–40). Another example is the family of aurein peptides from the Australian southern bell frogs *Litoria aurea* and *Litoria raniformis* (18,32,33,41), which is the focus of this contribution.

Submitted September 12, 2006, and accepted for publication January 4, 2007.

Yeang-Ling Pan and John T.-J. Cheng contributed equally to this work.

Address reprint requests to Suzana K. Straus, Tel.: 604-822-2537; Fax: 604-822-2157; E-mail: sstraus@chem.ubc.ca.

0006-3495/07/04/2854/11 $2.00

doi: 10.1529/biophysj.106.097238

Aurein peptides display a wide range of sequence diversity and activity with respect to Gram-positive bacteria (*Bacillus cereus*, *Leuconostoc lactis*, *Listeria innocua*, *Micrococcus luteus*, *Staphylococcus aureus*, and *Staphylococcus epidermidis*) and cancers (41). By far the most studied member of this family is aurein 1.2 (30,31,33,42,43). It is a 13-residue peptide with a net positive charge of +1. It possesses an amidated C-terminus ($CONH_2$ group) which increases the positive charge of the peptide, which in turn is deemed essential for its antibacterial action (18,32). It is most active against *L. lactis* (with a minimal inhibitory concentration (MIC) of 12 $\mu g.mL^{-1}$), followed by *S. aureus*, *S. epidermidis*, and *Streptococcus uberis* (with MICs of 50 $\mu g.mL^{-1}$) (41,44). Solution-state NMR and circular dichroism (CD) studies have shown that it adopts an α-helical conformation in membrane mimetic environments: 70% trifluoroethanol (TFE)/30% water (41) and sodium dodecyl sulfate micelles (45). Since, the length of aurein 1.2 is too short (~19.5 Å (29)) to span fluid lipid bilayers (~40 Å), it is proposed that this peptide interacts primarily with the membrane interface and promotes bilayer damage by a detergent-like or carpet-like mechanism. Another wide-spectrum antibiotic which behaves in exactly the same manner is citropin 1.1, a 16-residue peptide with a net +2 charge (18,32,33).

In this contribution, we report data on two 16-residue peptides from the aurein family: aurein 2.2 (net charge +2) and aurein 2.3 (net charge +2). Aurein 2.2 (Aur2.2-$CONH_2$) is active against a number of Gram-positive bacteria. For example, it displays a MIC of 25 $\mu g.mL^{-1}$ for *S. aureus* and *S. epidermidis* (41), i.e., it is more active than aurein 1.2 in this case and equally active to citropin 1.1. Aurein 2.3 (Aur2.3-$CONH_2$), on the other hand, is generally only marginally active, with typical MICs of 100 $\mu g.mL^{-1}$ (41). The difference in amino acid sequence between aurein 2.2 and 2.3 is only a conservative mutation of a leucine to an isoleucine at position 13. To assess how this mutation may be correlated to activity, we have determined the structure of Aur2.2-$CONH_2$ and Aur2.3-$CONH_2$ in TFE, in 1,2-dimyristoyl-*sn*-glycero-3-phosphocholine (DMPC) small unilamellar vesicles (SUVs), and in 1:1 DMPC/1,2-dimyristoyl-*sn*-glycero-3-[phospho-*rac*-(1-glycerol)] (DMPG) SUVs, using CD. The structures of the peptides in 25% TFE were also determined using solution-state ^{1}H-NMR. To further determine how activity is modulated by sequence, we have also studied a modified version of aurein 2.3 in which the amidated C-terminus is replaced by a carboxyl group (Aur2.3-COOH). In addition, we have determined the interaction of these three peptides with model zwitterionic (DMPC) membranes, using oriented CD and ^{31}P-solid-state NMR, to determine how they perturb the membrane bilayer. We have also determined how these peptides interact with bacterial model membranes consisting of a 1:1 mixture of DMPC/DMPG using oriented circular dichroism (OCD). Finally, we have tested the antibiotic activity of the three peptides against *S. Aureus* (strain C622, ATCC 25923) and *S. epidermidis* (strain C621—clinical isolate). Overall, these data should enable us to correlate structure and membrane interaction of these three marginally different peptides with antibiotic activity and lead to a better understanding of how sequence modulates function in the aurein peptide family.

MATERIALS AND METHODS

Materials

Fmoc-protected amino acids, Wang and Rink resin, and 2-(1H-benzotriazol-1-yl)-1,1,3,3-tetramethyluronium hexafluorophosphate (HBTU) were purchased from Advanced Chem Tech (Louisville, KY). *N*-Hydroxybenzotiazhole (HOBt) was obtained from Novabiochem (San Diego, CA). *N,N*-Dimethylformamide (DMF), dichloromethane (DCM), acetonitrile (AcN), and potassium nitrate were purchased from Fisher Chemicals (Nepean, Ontario, Canada). *N,N*-Diiopropylethylamine (DIEA), trifluoroacetic acid (TFA), ethane dithiol (EDT), and triethylsilane (TES) were obtained from Sigma-Aldrich (St. Louis, MO). Mylar plates were made by cutting Melinex Teijin films from Dupont (Wilton, UK). DMPC and DMPG were purchased from Avanti Polar Lipids (Alabaster, AL) and obtained dissolved in chloroform.

Methods

Peptide synthesis

Aurein 2.2 and aurein 2.3 (Aur2.3-$CONH_2$) were synthesized using Rink resin. Aur2.3-COOH was synthesized using Wang resin. In all cases, the synthesis was started by first precoupling the first residue (Fmoc-Leu) to the appropriate resin. Briefly, 0.30 mmol of the resin was presoaked for ~1 h in 10 mL DMF. Then Fmoc-Leu was preactivated by dissolving in 0.5 M DMF with 1 mmol HBTU, 1 mmol HOBT, and 2 mmol DIEA. The Fmoc-Leu was then added to the resin. The mixture was spun overnight.

Next, the peptides were synthesized using an Applied Biosystems 431A peptide synthesizer (Foster City, CA) by the in situ neutralization Fmoc chemistry, using the preloaded Leu-Wang resin or Leu-Rink resin, as appropriate. Side chains were protected as follows: Asp(OtBu), Lys(Boc), and Ser(tBu). For double coupling of serine, leucine, and isoleucine, one extra step of coupling was performed for each amino acid with only DMF washes in between. After chain assembly was completed, the peptide was deprotected and cleaved simultaneously from the resin using a cleavage mixture of 81% TFA, 5% ddH_2O, 2.5% EDT, and 1% TES for 5 h. TFA was then removed from the mixture by rotary evaporation. Chilled diethyl ether was used to precipitate the crude product. Finally, the resulting peptide was dissolved in water and lyophilized.

Purification

The crude peptide product was purified by preparative reverse-phase-high-performance liquid chromatography on a Waters 600 system (Waters Limited, Mississauga, Ontario, Canada) with 229-nm ultraviolet detection, using a Phenomenex (Torrance, CA) C4 preparative column (20 μm, 2.1 × 25 cm) at a flow rate of 20 mL/min and linear gradient of 0–50% buffer B (10% ddH_2O, 90% AcN containing 0.1% TFA) in buffer A (90% ddH_2O, 10% AcN containing 0.1% TFA) over 80 min. The identity of the products was verified using spectrometry: Aur2.2-$CONH_2$, purity ≥99%, molecular weight (MW) = 1615.0 (from matrix-assisted laser desorption ionization-time of flight (MALDI-TOF)); Aur2.3-$CONH_2$, purity ≥99%, MW = 1615.0 (from MALDI-TOF); Aur2.3-COOH, purity ≥98%, MW = 1616.0 (from MALDI-TOF).

Solution CD sample preparation

Solution CD samples with a constant peptide concentration of 200 μM were prepared in different compositions of water and TFE: 100% water, 75% water with 25% TFE, 50% water with 50% TFE, and 25% water with 75% TFE. Different peptide/DMPC and peptide/DMPC/DMPG lipid molar ratios of samples were also prepared: 1:15, 1:50, and 1:100. Appropriate amounts of lipids in chloroform were vacuum dried in a 25-mL round bottom flask overnight followed by addition of peptide in water. The mixture was sonicated in a water bath for at least 30 min (i.e., until the solution was no longer turbid) to ensure lipid vesicle formation. For all samples, corresponding background samples without peptides were prepared for spectral subtraction.

Solution NMR sample preparation

The peptides were dissolved in 65% water, 25% d_3-TFE, and 10% D_2O. Each peptide sample had a final concentration of 2 mM, with a total volume of 600 μL.

Mechanically oriented sample preparation

For solid-state NMR analysis, samples were prepared for four different peptide/DMPC lipid molar ratios of 1:15, 1:30, 1:40, and 1:120. The amount of DMPC (dissolved in chloroform) was kept constant at 19.18 μmol. The lipid was dried using a stream of air to remove most of the chloroform. Then, the appropriate amount of peptide was added and the mixture was redissolved in 800 μL of methanol. The mixture was deposited in 5-μL portions repeatedly onto nine Mylar plates, which were placed in a petri dish. Between depositions, most of the methanol evaporated before the next portion was deposited onto the plate. The plated samples were then covered and left to dry overnight on the bench. The slides, on which the samples were still slightly humid ($\sim$1 μl of water per slide), were stacked. Next, the samples were placed in a 93% relative humidity chamber and were indirectly hydrated by incubating inside the desiccator at 37°C for 4 days. The humidity of the samples was verified by visual inspection. The degree of alignment was verified by ^{31}P-solid-state NMR. Consistent sample preparation was verified by preparing 2–3 samples for each lipid composition and peptide concentration. Finally, the plated samples were wrapped in a thin layer of parafilm before data acquisition.

For oriented CD analysis, samples were prepared in a similar fashion as described above. The peptide amount was kept constant at 0.5 μmol and mixed with appropriate molar ratios of DMPC or DMPC/DMPG and sonicated in 2 mL of methanol. Each mixture was deposited in 90-μL portions with a syringe onto 3 $\times$ 1 cm and 1-mm-thick quartz slides, which were cleaned thoroughly with ethanol. After indirect hydration of the samples, clear layers of samples were obtained on the slides. Each sample was covered with a second slide with a spacer in between. Spacers were made by cutting six layers of stacked parafilm into a rectangular 3 $\times$ 1 cm frame with 2-mm width. To hold the slides in place, a thin layer of parafilm was wrapped around the edges of the slides.

Circular dichroism

CD experiments were carried out using a JASCO J-810 spectropolarimeter (Victoria, British Columbia, Canada) at 30°C. The spectra were obtained over a wavelength range of 185–250 nm. Continuous scanning mode with a response of 1 s with 0.5-nm steps, bandwidth of 1.5 nm, and a scan speed of 20 nm/min were used. The signal/noise ratio was increased by acquiring each spectrum over an average of three scans. Finally, each spectrum was corrected by subtracting the background from the sample spectrum. Solution CD samples were placed in a cell (0.1 cm in length) in 200-μL portions, whereas oriented CD samples on quartz slides were directly placed in the sample compartment. The temperature was kept constant by means of a water bath.

NMR spectroscopy

Solution-state NMR data were acquired on a Bruker 500-MHz instrument (Milton, Ontario, Canada), operating at a ^{1}H frequency of 500.17 MHz. The parameters for the experiments were chosen to match previously reported parameters for aurein 1.2 (43) as much as possible. All spectra were collected at 25°C. Spectra were acquired using total correlation spectroscopy (TOCSY) and nuclear Overhauser enhancement spectroscopy (NOESY) experiments in phase-sensitive mode using time proportional phase incrementation (TPPI) (46) in the indirect dimension. The TOCSY experiment used the MLEV17 sequence for mixing (mixing time = 70 ms) and excitation sculpting with gradients for water suppression (47). The two-dimensional data set consisted of 4096 data points in t_2 and 256 points in t_1. The NOESY experiment was acquired with a mixing time of 150 ms and also used excitation sculpting for water suppression. The data size for this data set was the same as for the TOCSY spectrum. Signals were averaged using 32 scans for the TOCSY and 64 scans for the NOESY experiments, respectively. The spectra were referenced to the residual methylene protons present in d_3-TFE (3.918 ppm). Spectra were processed to result in 1k $\times$ 1k points.

^{31}P-solid-state NMR experiments on mechanically aligned DMPC samples were carried out on the same Bruker 500-MHz NMR spectrometer, operating at a phosphorus frequency of 202.48 MHz. ^{31}P-NMR spectra were obtained at 30°C with a single ^{31}P-pulse/^{1}H-decoupling sequence where the decoupling was achieved using SPINAL-16 (48). The 90° pulse was set to 9.75 μs and a 3-s recycle delay was used. Each spectrum was acquired using 2048 scans, with no line broadening applied.

Minimal inhibitory concentration determination

MIC for Aur2.2-$CONH_2$, Aur2.3-$CONH_2$, and Aur2.3-COOH were determined based on the previously described modified methodology (49). Briefly, 18-h cultures of *S. aureus* C622 (ATCC 25923) and *S. epidermidis* C621 (clinical isolate generously donated by D. Speert) grown in Mueller Hinton (MH) medium (Difco, Oakville, Ontario, Canada) were diluted to $\sim 2 \times 10^5$ colony forming units per mL. Then 90 μL of diluted culture was dispensed into a 96-well polystyrene microtitre plate (Costar, Cambridge, MA). Separately, twofold serial dilutions in sterile MH broth of the respective peptide were carried out at 10$\times$ final concentration before 10 μL of each dilution was transferred to the culture and grown for 18 h at 37°C before being read. The MIC was recorded as the lowest concentration of peptide in which no visible growth could be observed. Controls included the peptide antibiotic polymyxin B (Sigma, St. Louis, MO). In addition, culture-only and broth-only wells were used.

RESULTS

Structure determination of aurein peptides by CD and solution-state NMR

To determine which structure the Aur2.2-$CONH_2$, Aur2.3-$CONH_2$, and Aur2.3-COOH peptides adopt in water and in the presence of model membranes, solution CD experiments were performed. Fig. 1 shows that all three peptides adopt a random coil conformation in aqueous solution (Fig. 1, *a–c*, *solid black line*). Upon addition of TFE, all three peptides change conformation. Spectra consisting of a peak at 190 nm and two minima at 210 nm and 222 nm, which are characteristic of α-helical structure, are observed for all TFE concentrations (25%, 50%, and 75%) and all peptides. As TFE has been shown to promote the formation of α-helices (for a recent example, see Perham et al. (50)), CD spectra of the Aur2.2-$CONH_2$, Aur2.3-$CONH_2$, and Aur2.3-COOH

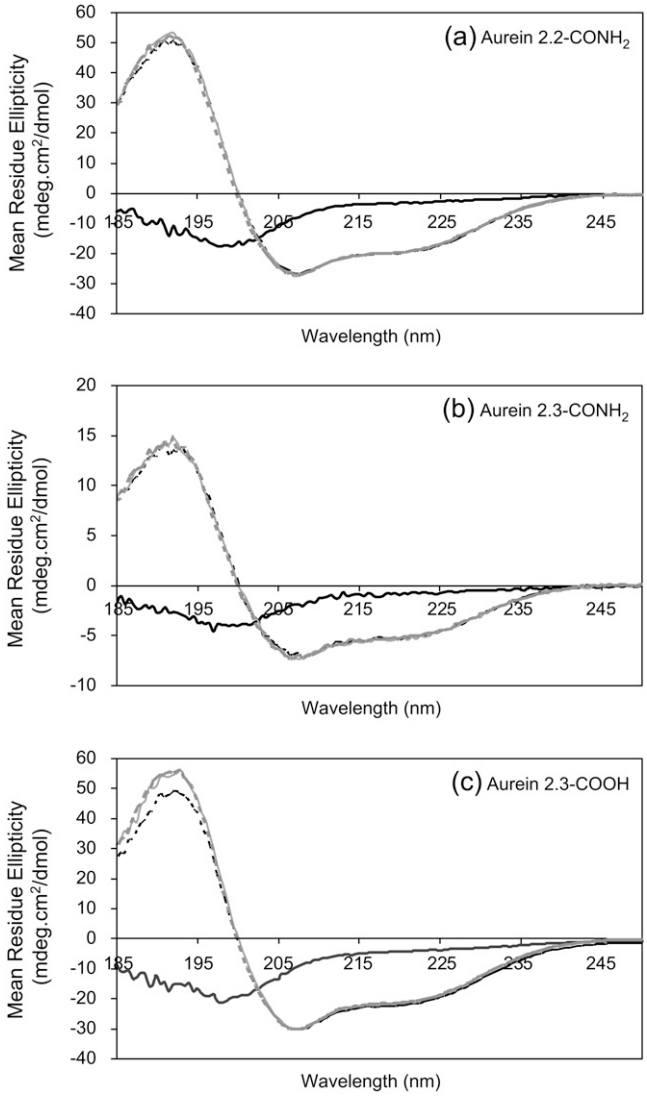

FIGURE 1 Solution CD spectra of the aurein peptides in water/TFE mixtures: (*a*) Aur2.2-$CONH_2$, (*b*) Aur2.3-$CONH_2$, and (*c*) Aur2.3-COOH (*solid black line*, 100% H_2O; *black dotted line*, 75% H_2O/25% TFE; *solid gray line*, 50% H_2O/50% TFE; *gray dotted line*, 25% H_2O/75% TFE). The spectra indicate that, in all cases, the peptides are unstructured in water but adopt an α-helical conformation upon addition of TFE.

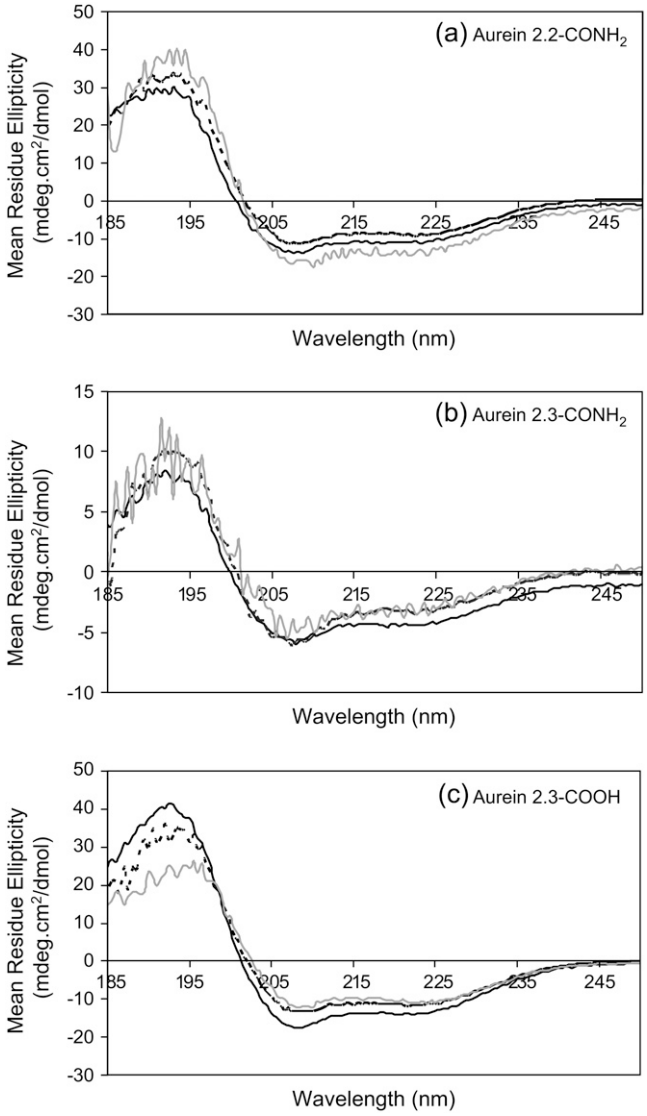

FIGURE 2 Solution CD spectra of the aurein peptides in DMPC SUVs: (*a*) Aur2.2-$CONH_2$, (*b*) Aur2.3-$CONH_2$, and (*c*) Aur2.3-COOH (*solid black line*, P/L = 1:15; *dotted line*, P/L = 1:50; *solid gray line*, P/L = 1:100). The spectra indicate that the peptides adopt an α-helical conformation in the presence of DMPC SUVs.

peptides were also determined in DMPC and DMPC/DMPG (1:1) SUVs to determine the true conformation in a membrane environment. The spectra, illustrated in Figs. 2, *a–c*, and 3, *a–c*, respectively, demonstrate that the aurein peptides also adopt an α-helical conformation in this case. Similar intensities were observed for all the peptide/lipid molar ratios (P/L = 1:15, 1:50, and 1:100) studied here. This indicates that maximum binding of the peptide to the vesicles occurred. Evidence for saturation would manifest itself in a change in the CD signal, due to the contribution to the signal from an increased proportion of random coil structure (33).

To determine whether the peptides adopt a continuous α-helical structure or whether the peptides are bent, ^{1}H-solution-state NMR experiments were performed. As no changes in the CD spectra were observed in the TFE concentration range used here, the solution-state NMR spectra were collected using 25% d_3-TFE. The ^{1}H-NMR spectra for the three peptides were assigned using the TOCSY and NOESY data sets, using TOPSPIN. Of all three peptides, the spectra for Aur2.3-$CONH_2$ were the least overlapped. The assignments (not shown) did not vary significantly from peptide to peptide, giving us a first indication that the peptides all adopt similar structures. In the H^N-H^N region (not shown) and in the fingerprint region (Fig. 4, *a–c*), a large number of sequential (*i* to *i* + 1) connectivities were observed. At a low contour level, additional *i* to *i* + 2 connectivities were observed in the

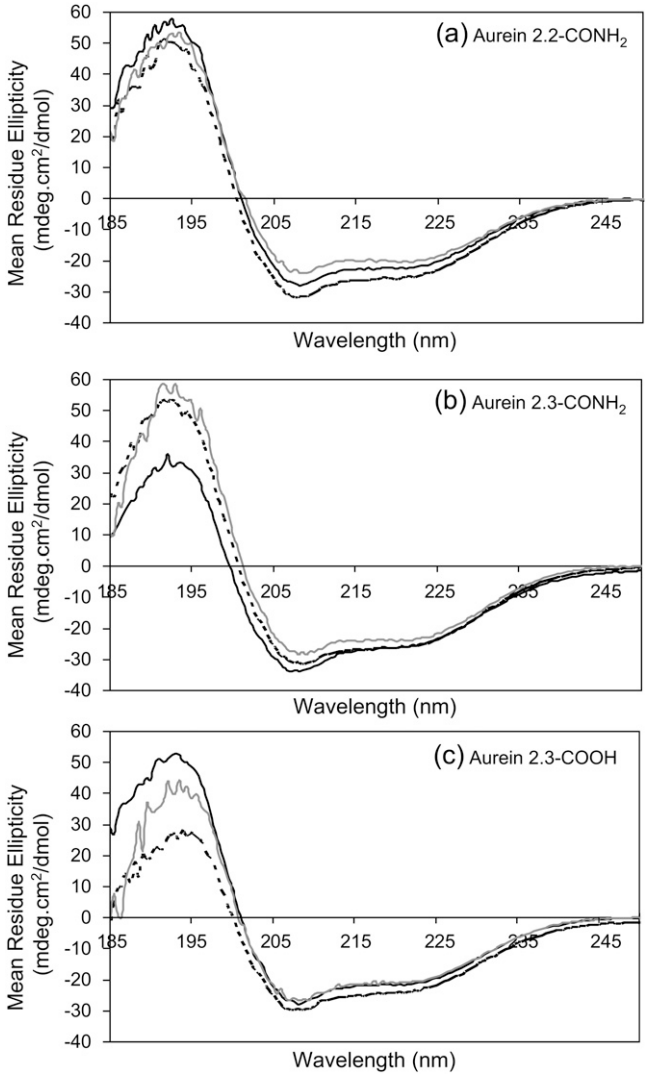

FIGURE 3 Solution CD spectra of the aurein peptides in DMPC/DMPG (1:1) SUVs: (*a*) Aur2.2-$CONH_2$, (*b*) Aur2.3-$CONH_2$, and (*c*) Aur2.3-COOH (*solid black line*, P/L = 1:15; *dotted line*, P/L = 1:50; *solid gray line*, P/L = 1:100). The spectra indicate that the peptides adopt an α-helical conformation in the presence of DMPC/DMPG SUVs.

H^N-H^N region, as summarized in Fig. 5 *b* for Aur2.3-$CONH_2$. Other nuclear Overhauser enhancement (NOE) connectivities observed include $d_{\alpha N}(i,i+4)$, $d_{\alpha N}(i,i+3)$, and $d_{\alpha\beta}(i,i+3)$, as summarized in Fig. 5 *b*. These data as well as the observed chemical shift differences of the measured H^α chemical shifts with respect to random coil values (51) (Fig. 5 *a*) suggest that all three peptides adopt a continuous α-helical structure. Full structure calculations (not performed at this time) could be used to further confirm these results.

Membrane interaction of aurein peptides by oriented CD and ^{31}P-solid-state NMR

To determine how the Aur2.2-$CONH_2$, Aur2.3-$CONH_2$, and Aur2.3-COOH peptides interact with membrane bilayers, OCD and ^{31}P-solid-state NMR experiments were carried out. For both methods, samples were prepared in almost identical fashion so that the data sets could be compared directly and also to verify that the samples were aligned. All experiments were conducted at 30°C, i.e., in the liquid crystalline phase for DMPC/DMPG. In addition, experiments were repeated at least twice, using at least two different samples (for each concentration), to ensure reproducibility of the results. The OCD results for the Aur2.2-$CONH_2$, Aur2.3-$CONH_2$, and Aur2.3-COOH peptides in DMPC and DMPC/DMPG (1:1) bilayers are shown in Fig. 6. The spectra were scaled so that the minimum at 222 nm has the same intensity. The data illustrate that at a peptide/lipid (P/L) molar ratio of 1:15, all peptides are no longer completely in the surface-adsorbed or S state (52,53) in DMPC (Fig. 6, *a–c*). In fact, at this P/L ratio, the peptides can be seen as either i), being in the inserted or I state with a tilt angle (33,54)—also known as the tilted or T-state (55); or ii), being 50% oriented transmembrane and 50% surface adsorbed (53). As the peptide is too short to span the membrane bilayer entirely, since its hydrophobic length is ~24 Å and the DMPC bilayer hydrophobic thickness is 26.5 Å (12,56) in the liquid crystalline phase, it is quite likely that the peptide is inserted at an angle at P/L = 1:15. The critical threshold peptide concentration (P/L*) is between 1:15 and 1:30 for the amidated peptides, whereas it is between 1:30 and 1:40 for Aur2.3-COOH. These threshold concentrations are similar to those observed for aurein 1.2 and citropin 1.1 (33), where a change is observed to occur between P/L molar ratios of 1:50 and 1:15. Interestingly, the Aur2.3-COOH peptide, which is presumably the least active of the three peptides, appears to insert into phosphatidylcholine (PC) bilayers slightly more readily than its amidated C-terminus counterpart. In DMPC/DMPG bilayers (Fig. 6, *d–f*), the amidated peptides insert at all concentration ranges shown, i.e., for P/L ratios of 1:120–1:15. Indeed, even at very low peptide concentrations (P/L ~ 1:200), Aur2.2-$CONH_2$ and Aur2.3-$CONH_2$ remain in the I-state (data not shown). For the Aur2.3-COOH peptide, on the other hand, the threshold P/L* concentration is between 1:80 and 1:120, indicating that comparatively high peptide concentrations are needed for insertion to take place. This is most likely due to the unfavorable electrostatic interactions between the negatively charged C-terminus and the negatively charged PG headgroups (57).

^{31}P-NMR spectra (shown in Fig. 7) were recorded for all peptides in DMPC. The spectra, acquired with the membrane normal parallel to the magnetic field, illustrate that for the most part, the lipids remain aligned with increasing peptide concentration. The peptides appear to disorder the headgroups somewhat, as evidenced by the scaling of the ^{31}P-chemical-shielding anisotropy. In addition, the peptides affect the dynamics of the lipid headgroups, as shown by a decrease in T_2, leading to line broadening. Both these effects have also been previously observed for aurein 1.2 and citropin 1.1 (31). In addition, a small proportion of the lipid headgroups

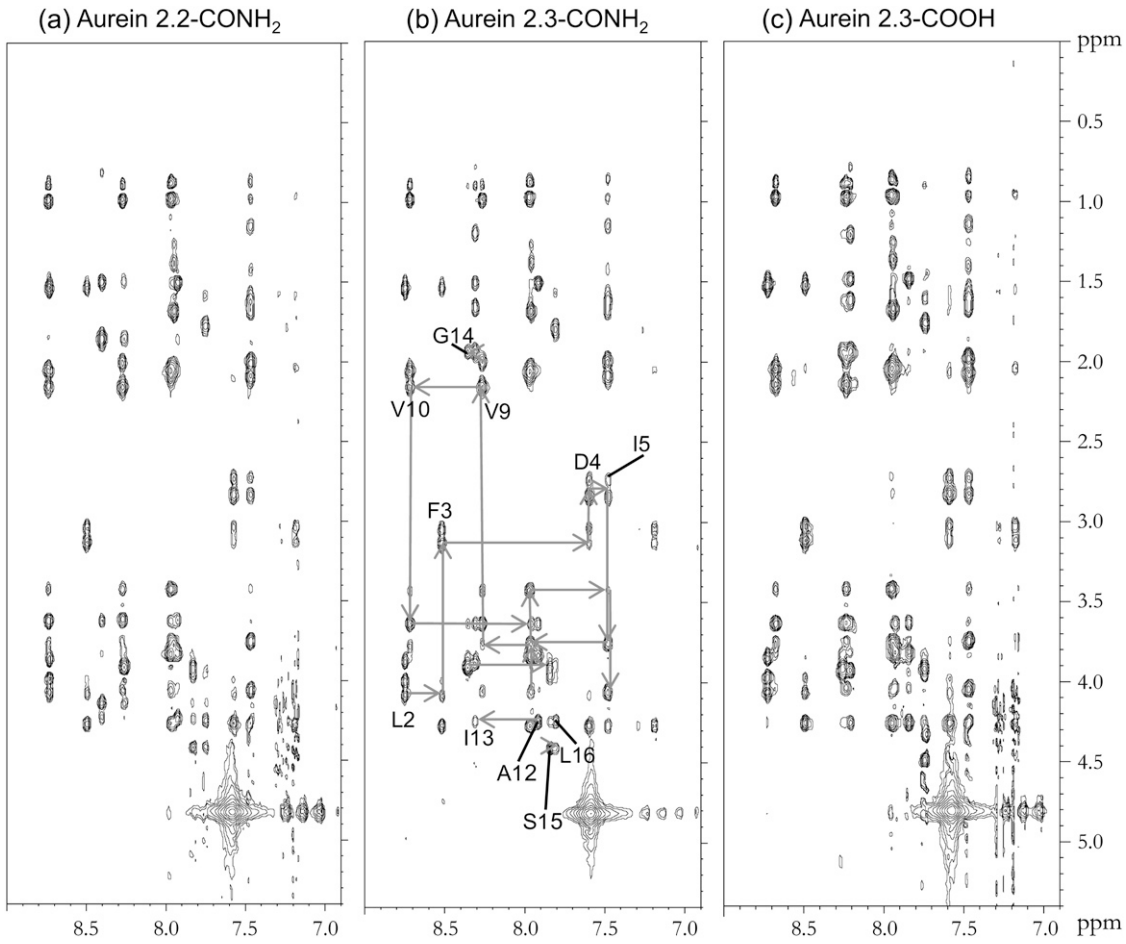

FIGURE 4 Fingerprint region of solution NMR NOESY spectra of (*a*) Aur2.2-$CONH_2$, (*b*) Aur2.3-$CONH_2$, and (*c*) Aur2.3-COOH. The spectra were acquired using a phase-sensitive NOESY experiment, with excitation sculpting with gradients for water suppression (see text). All spectra were acquired at 25°C, using 64 scans and a mixing time of 150 ms. The spectra were referenced to the residual methylene protons present in d3-TFE (3.918 ppm). In *b*, arrows indicate some of the connectivities use to perform the sequential assignment. In ambiguous cases, the HN-HN region was also used to confirm *i* to $i + 1$ connectivities.

are significantly perturbed, as seen by the appearance of an additional ^{31}P-NMR resonance (at 12 ppm) with increasing peptide concentration. The presence of a peak near the isotropic position has previously been observed in ^{31}P-NMR spectra of aurein 1.2 and has been attributed to membrane disruption (31). Generally, the presence of a peak at or near the isotropic position has been observed in solid-state NMR studies of other antimicrobial peptides (26,58–60) and has been attributed to the formation of small lipid vesicles/micelles, the formation of a different lipid phase (26), or toroidal pore defects within the bilayer (59,61). To clearly identify which of these mechanisms is relevant here, additional data from experiments such as differential scanning calorimetry (to determine changes in phase) or ^{15}N-NMR (to determine the orientation of the peptide in the bilayer) would be needed. As the aim of this study was to determine whether the aurein peptides studied here behave differently to aurein 1.2 and citropin 1.1 (which promote bilayer damage via a detergent-like mechanism (16), resulting in turn in membrane leakage (30)) and to determine whether this can be correlated to activity, the exact nature of the manner in which Aur2.2-$CONH_2$, Aur2.3-$CONH_2$, and Aur2.3-COOH perturb DMPC membranes will not be characterized further at this point in time. The ^{31}P-NMR data suggest in corroboration with the OCD results that the interaction of these three peptides with DMPC bilayers is identical.

Antibiotic activity of the aurein peptides

Given that all three peptides studied here adopt α-helical structure regardless of membrane environment (DMPC versus DMPC/DMPG) and given that the peptides interact with the membranes in a manner which cannot be directly correlated to activity, MICs of all three peptides against two Gram-positive bacteria (*S. aureus* and *S. epidermidis*) were determined. The MICs, reported in Table 1, indicate that the amidated peptides have very similar activities under conditions used here, contrary to what is reported in the literature

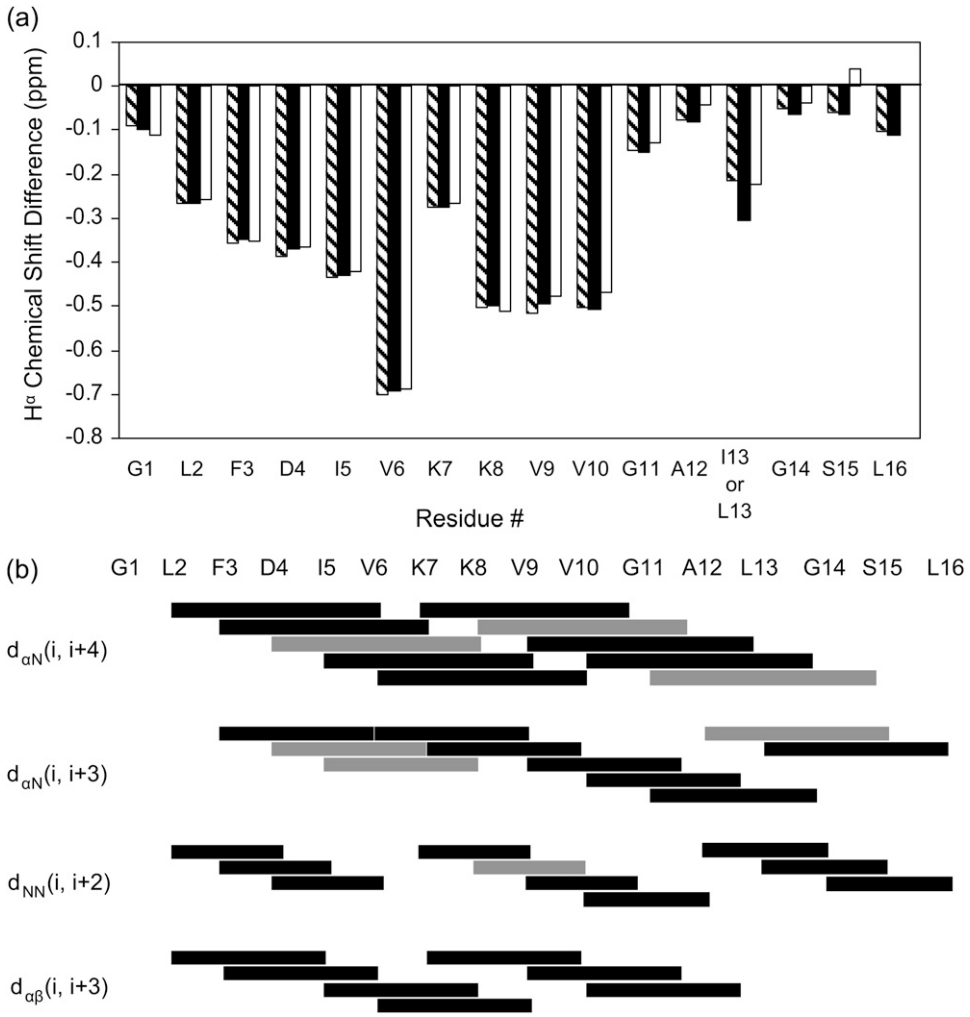

FIGURE 5 NMR-derived evidence indicating that the aurein peptides are α-helical: (*a*) Hα chemical shift differences for Aur2.2-$CONH_2$ (*hashed*), Aur2.3-$CONH_2$ (*solid black*), and Aur2.3-COOH (*open*); (*b*) typical NOE connectivities observed for these peptides—shown here for Aur2.3-$CONH_2$ only. Solid black bars represent unambiguous NOEs, and gray bars represent connectivities which are present but are ambiguous due to overlap.

(41). Aur2.2-$CONH_2$ and Aur2.3-$CONH_2$ have similar MICs of 15 μg.mL^{-1} and 25 μg.mL^{-1}, respectively, against the wild-type *S. aureus* strain C622. Likewise, these two peptides have identical MICs of 8 μg.mL^{-1} against *S. epidermidis* strain C621. The COOH version of aurein 2.3, on the other hand, is not active with MICs of >100 μg.mL^{-1} for both types of bacteria. Peptides with charged C-termini have been found to be inactive or much less active (18,41) than their amidated counterparts. Wells containing polymyxin B, culture only, and broth only were used as controls. The MICs observed for polymyxin B are reported in Table 1 and agree with literature findings (62).

DISCUSSION

Determining the structure of antimicrobial peptides and characterizing their interaction with lipid bilayers is essential to understanding how they function and kill bacteria. By elucidating the mode of action of antibiotics, it is possible to, on the one hand, better understand how microbes develop resistance (5), and on the other, develop modified versions of these agents to mitigate this development. An approach which has received much attention recently is to search for naturally occurring antibiotic molecules derived from the plant and animal kingdoms (1,3,15,16,63), which have net positive charge and typically adopt amphiphilic structures to maximize their interactions with bacterial membranes.

To elucidate the mode of action of a cationic antimicrobial peptide, one typically picks a highly active peptide and determines i), its structure by CD and/or NMR in a membrane or membrane mimetic environment, and ii), its interaction with model membrane bilayers such as 1-palmitoyl-2-oleoyl-*sn*-glycero-3-phosphocholine (POPC) (e.g., MSI-78 and MSI-594 (64)), DPhPC (e.g., alamethicin (61,65)), DMPC (e.g., aurein 1.2 (33)), and other diacylphosphatidylcholine membranes (e.g., $K_2(LA)_xK_2$ (66)), i.e., lipids which are good models for probing the hemolytic activity of the peptides, or lipid mixtures, such as POPC/PG (e.g., MSI-78 and MSI-594 (64)) and DMPC/DMPG (e.g., PGLa (55)), i.e., bacterial model membranes. To completely describe the peptide-lipid interactions, one needs to take into account a range of parameters such as peptide/lipid ratio, membrane composition,

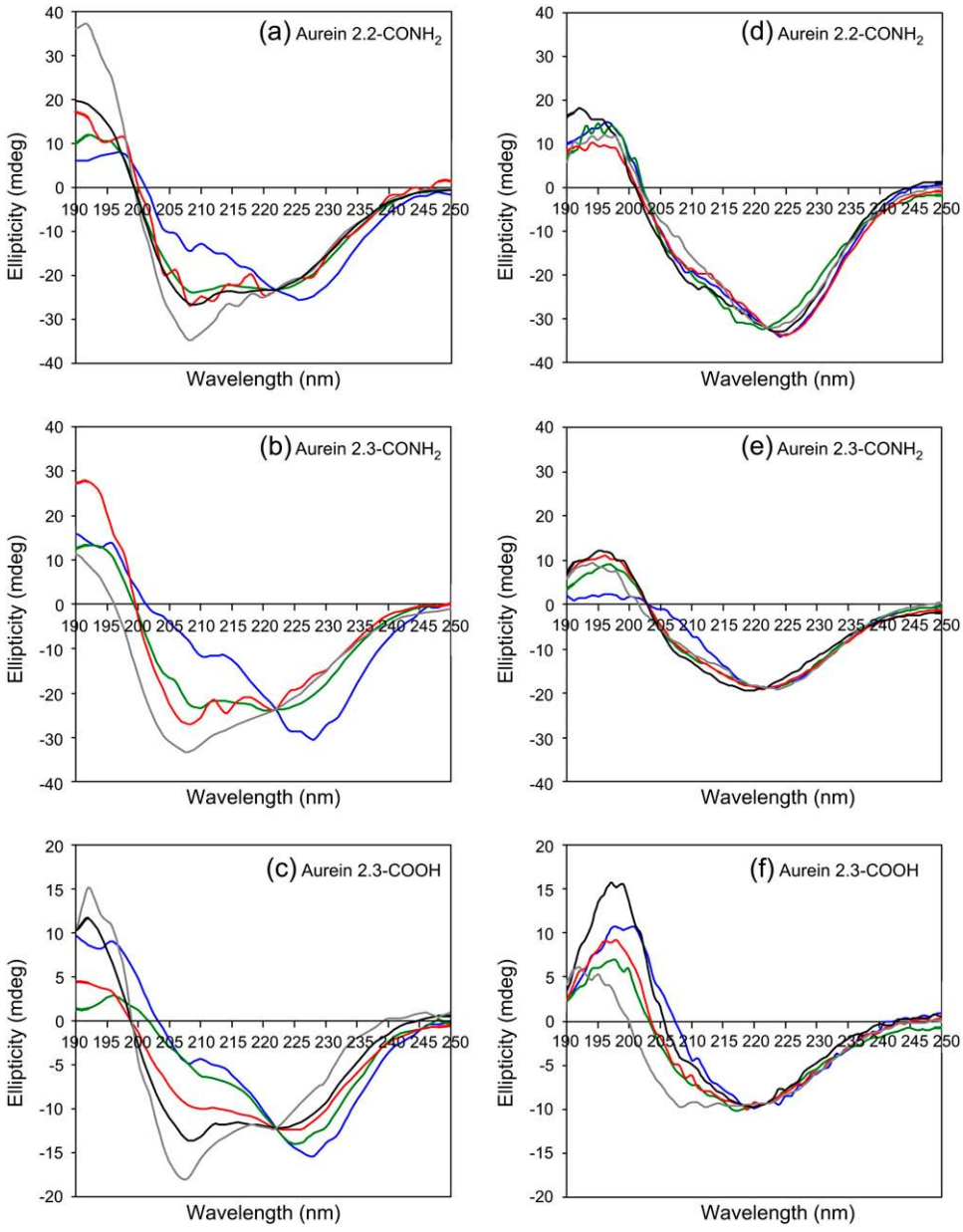

FIGURE 6 Oriented CD spectra for (*a*) Aur2.2-$CONH_2$, (*b*) Aur2.3-$CONH_2$, and (*c*) Aur2.3-COOH in DMPC and (*a*) Aur2.2-$CONH_2$, (*b*) Aur2.3-$CONH_2$, and (*c*) Aur2.3-COOH in DMPC/DMPG (1:1). P/L molar ratios = 1:15 (*blue*), 1:30 (*green*), 1:40 (*red*), 1:80 (*black*), and 1:120 (*gray*). The spectra were normalized such that the intensities of all spectra at 222 nm are the same. The spectra show that the peptides insert into the DMPC bilayer at threshold P/L* molar ratios between 1:15 and 1:30 for Aur2.2-$CONH_2$ and Aur2.3-$CONH_2$, and 1:30 and 1:40 for Aur2.3-COOH. In DMPC/DMPG (1:1), the amidated peptides are inserted over the entire concentration range, whereas the P/L* is between 1:120 and 1:80 for Aur2.3-COOH under these conditions.

temperature, hydration, buffer composition (16), and lipid phase (61). Once this is taken into consideration, one typically generates a model by which the peptide inserts into the lipid bilayer: via the carpet mechanism (6), barrel-stave (10) or toroidal (67) pore formation, or simply a detergent-like mechanism (16,23), as previously mentioned.

Here we have taken a slightly different approach in that we have studied three peptides which have essentially the same amino acid sequence but have very different reported activities (41) with respect to different microbes. Aurein 2.2 (GLFDIVKKVVGALGSL-$CONH_2$) is reported to be the most active of the three peptides investigated. It shares its first 9 residues in common with citropin 1.1 (though 2 residues have slightly different order), which is also 16 amino acid residues in length. Presumably this sequence similarity may explain why Aur2.2-$CONH_2$ and citropin 1.1 display similar activities against *L. lactis*, *S. aureus*, and *S. epidermidis* (43). Aurein 2.3, on the other hand, with a single point mutation L-13 → I-13, is only marginally active (41). We also investigated a modified version of aurein 2.3, with a carboxy C-terminus. Since most active members of the aurein peptide family have an amidated C-terminus, with only one aurein (aurein 5.2) with a −COOH terminus being active, and then only marginally so (43), it is expected that Aur2.3-COOH will at best be only marginally active.

The data presented here show that despite the difference in sequence and in reported activity, all three peptides adopt continuous α-helical structures. The results from solution

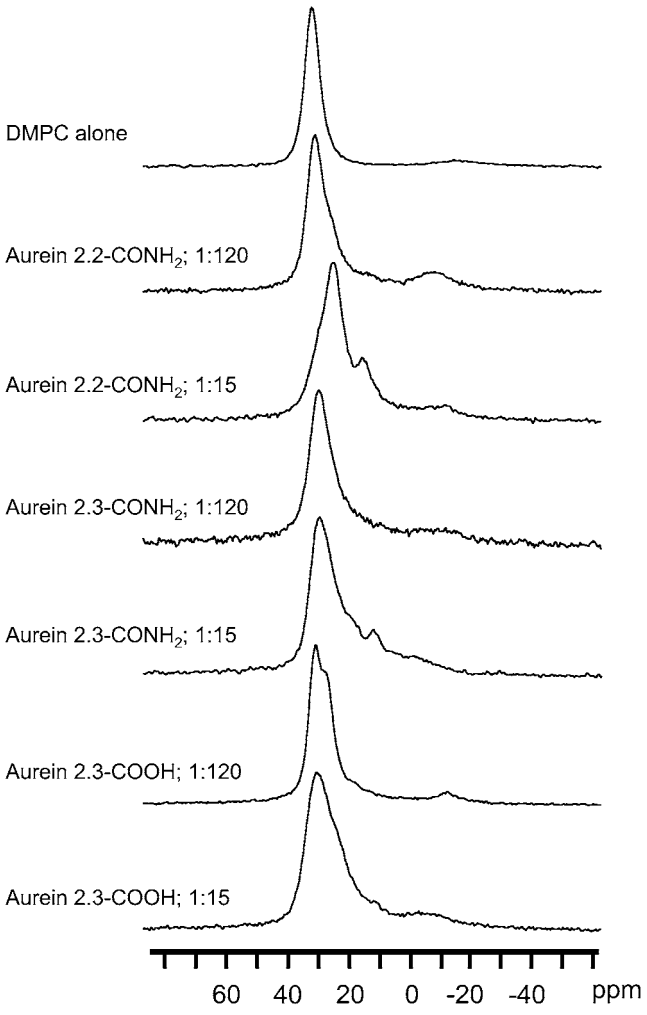

FIGURE 7 ^{31}P-solid-state NMR spectra of all three aurein peptides oriented in DMPC bilayers. The spectra were recorded using 2048 scans at 30°C, oriented such that the membrane normal was parallel to the external magnetic field. The spectra were processed without any line broadening (see text for further experimental details).

CD and NMR are, in fact, analogous to those reported in the literature for aurein 1.2 and citropin 1.1 (33,43). In all cases, these antimicrobial peptides are unstructured in solution and then fold in the presence of membranes or membrane mimetics. In other words, all peptides follow the first step of the Shai-Matsuzaki-Huang model (6–10) regardless of whether the peptides are in TFE, DMPC SUVs, or DMPC/DPMG (1:1) SUVs. Once folded, the aurein peptides studied here then interact with PC membranes by predominantly associating with the surface. At high concentrations, the peptides realign from a surface-bound S-state to a tilted T-state (i.e., insert at a tilt angle). The exact value of this tilt angle has yet to be determined (e.g., by labeling one residue with ^{15}N (31,33)) but is expected to be similar to that of citropin 1.1 (33), given the same length of the peptides. The transition from the S to the T state occurs at P/L* between 1:15 and 1:30 for the amidated peptides and between 1:30 and 1:40 for Aur2.3-COOH. The slightly more favorable insertion of Aur2.3-COOH into PC membranes is most likely due to electrostatic interactions (57). Repulsive interactions between C-termini which are in proximity when the peptide is surface associated are presumably minimized when the peptides insert. The ^{31}P-NMR spectra of aligned peptides in DMPC show that at high peptide concentrations, a proportion of the lipid headgroups are perturbed. This is again similar to what was observed for aurein 1.2 and citropin 1.1 (31). The similar OCD and NMR spectra observed for all peptides suggest that the interaction of the aurein peptides with PC membranes does not depend on sequence or the nature of the C-terminus. The interactions of the aurein peptides with bacterial model membranes consisting of DMPC/DMPG (1:1), on the other hand, show that the nature of the C-terminus modulates peptide insertion. Aur2.2-$CONH_2$ and Aur2.3-$CONH_2$ display similar behavior and insert readily into PC/PG membranes, even at low peptide concentrations (i.e., P/L* $<$ 1:200). The Aur2.3-COOH peptide inserts into PC/PG membranes at P/L* between 1:120 and 1:80. In other words, it inserts more readily into PC/PG membranes than in PC alone but does not insert as easily as the amidated peptides do. Clearly, the charge interactions between the positively charged Lys side chains and the negatively charged lipid headgroups drive all the aurein peptides to interact with and insert more readily in PC/PG bilayers. The charge repulsions between the COOH terminus and the PG headgroups result in higher Aur2.3-COOH peptide concentration needed for the T state to be achieved.

Overall, the structural and membrane interaction data indicate that the single point mutation L-13 → I-13 in going from Aur2.2-$CONH_2$ to Aur2.3-$CONH_2$ does not affect how these peptides fold and interact with DMPC and DMPC/DMPG membranes. This is consistent with the new activity measurements reported here, which show that these two peptides have similar bactericidal properties. This indicates that small changes in the overall hydrophobicity of a peptide (i.e., leucine and isoleucine have slightly different hydrophobicity scales (68)) are not likely to have an effect on the activity of a cationic antimicrobial peptide. In addition, the data indicate that the nature of the C-terminus, specifically its charge, does not affect the structure a cationic antimicrobial

TABLE 1 MICs in μg.mL^{-1} of Aur2.2-$CONH_2$, Aur2.3-$CONH_2$, Aur2.3-COOH, and polymyxin B (control) toward *S. aureus* and *S. epidermidis* (see text for experimental details)

Peptide	*S. aureus* strain C622	*S. aureus* (41)	*S. epidermidis* strain C621	*S. epidermidis* (41)
Aur2.2-$CONH_2$	15	25	8	25
Aur2.3-$CONH_2$	25	100	8	100
Aur2.3-COOH	≥100	–	>128	–
Polymyxin B	50	–	55	–

MICs are given as the most frequently observed value obtained from repeat experiments.

peptide adopts in the presence of membrane but rather its interaction with charged lipid headgroups. The MICs obtained for the Aur2.3-COOH peptide clearly show that a charged C-terminus can destroy the antibiotic activity.

In conclusion, we have demonstrated that to elucidate the mode of action of a family of cationic antimicrobial peptides, it may be useful to compare peptides with similar sequences but different activities to determine whether structure and/or membrane interactions are important for activity. We have also shown that it is important to study these peptides in bacterial model membranes (DMPC/DMPG) and not DMPC alone, as electrostatic interactions are an important driving force for peptide-lipid interactions. Finally, now that we have determined under which conditions the Aur2.2-$CONH_2$ and Aur2.3-$CONH_2$ peptides perturb lipid bilayers and how that is correlated with activity, we will determine the exact mechanism by which these peptides bring about membrane disruption. We will verify whether the detergent-like mechanism proposed for aurein 1.2 and citropin 1.1 based on data obtained in DMPC (31,33) is also relevant for the aurein 2.2 and 2.3 peptides studied here.

The CD/OCD measurements were performed at the University of British Columbia Centre for Biological Calorimetry (CBC).

S.K.S. acknowledges financial support from the Natural Science and Engineering Research Council of Canada (Discovery Grant and University Faculty Award) and University of British Columbia, as well as funding from the Canada Foundation for Innovation for purchase of the 500-MHz NMR spectrometer used in this work.

REFERENCES

1. Hancock, R. E. W. 2001. Cationic peptides: effectors in innate immunity and novel antimicrobials. *Lancet Infect. Dis.* 1:156–164.
2. Zasloff, M. 2002. Antimicrobial peptides of multicellular organisms. *Nature*. 415:389–395.
3. Hancock, R. E. W. 2005. Mechanisms of action of newer antibiotics for Gram-positive pathogens. *Lancet Infect. Dis.* 5:209–218.
4. Devine, D. A., and R. E. W. Hancock. 2002. Cationic peptides: distribution and mechanisms of resistance. *Curr. Pharm. Des.* 8:703–714.
5. Peschel, A., and H. G. Sahl. 2006. The co-evolution of host cationic antimicrobial peptides and microbial resistance. *Nat. Rev. Microbiol.* 4:529–536.
6. Shai, Y. 1999. Mechanism of the binding, insertion and destabilization of phospholipid bilayer membranes by alpha-helical antimicrobial and cell non-selective membrane-lytic peptides. *Biochim. Biophys. Acta.* 1462:55–70.
7. Papo, N., and Y. Shai. 2005. Host defense peptides as new weapons in cancer treatment. *Cell. Mol. Life Sci.* 62:784–790.
8. Matsuzaki, K. 1999. Why and how are peptide-lipid interactions utilized for self-defense? Magainins and tachyplesins as archetypes. *Biochim. Biophys. Acta.* 1462:1–10.
9. Yang, L., T. M. Weiss, R. I. Lehrer, and H. W. Huang. 2000. Crystallization of antimicrobial pores in membranes: magainin and protegrin. *Biophys. J.* 79:2002–2009.
10. Huang, H. W. 2000. Action of antimicrobial peptides: two-state model. *Biochemistry.* 39:8347–8352.
11. Mecke, A., D. K. Lee, A. Ramamoorthy, B. G. Orr, and M. M. Holl. 2005. Synthetic and natural polycationic polymer nanoparticles interact selectively with fluid-phase domains of DMPC lipid bilayers. *Langmuir.* 21:8588–8590.
12. Mecke, A., D. K. Lee, A. Ramamoorthy, B. G. Orr, and M. M. Banaszak Holl. 2005. Membrane thinning due to antimicrobial peptide binding: an atomic force microscopy study of MSI-78 in lipid bilayers. *Biophys. J.* 89:4043–4050.
13. Chen, F. Y., M. T. Lee, and H. W. Huang. 2003. Evidence for membrane thinning effect as the mechanism for peptide-induced pore formation. *Biophys. J.* 84:3751–3758.
14. Wu, M., E. Maier, R. Benz, and R. E. W. Hancock. 1999. Mechanism of interaction of different classes of cationic antimicrobial peptides with planar bilayers and with the cytoplasmic membrane of Escherichia coli. *Biochemistry.* 38:7235–7242.
15. Hancock, R. E. W., and D. S. Chapple. 1999. Peptide antibiotics. *Antimicrob. Agents Chemother.* 43:1317–1323.
16. Bechinger, B., and K. Lohner. 2006. Detergent-like actions of linear amphipathic cationic antimicrobial peptides. *Biochim. Biophys. Acta.* 1758:1529–1539.
17. Straus, S. K., and R. E. Hancock. 2006. Mode of action of the new antibiotic for Gram-positive pathogens daptomycin: comparison with cationic antimicrobial peptides and lipopeptides. *Biochim. Biophys. Acta.* 1758:1215–1223.
18. Pukala, T. L., J. H. Bowie, V. M. Maselli, I. F. Musgrave, and M. J. Tyler. 2006. Host-defence peptides from the glandular secretions of amphibians: structure and activity. *Nat. Prod. Rep.* 23:368–393.
19. Rinaldi, A. C. 2002. Antimicrobial peptides from amphibian skin: an expanding scenario. *Curr. Opin. Chem. Biol.* 6:799–804.
20. Giovannini, M. G., L. Poulter, B. W. Gibson, and D. H. Williams. 1987. Biosynthesis and degradation of peptides derived from Xenopus laevis prohormones. *Biochem. J.* 243:113–120.
21. Zasloff, M. 1987. Magainins, a class of antimicrobial peptides from Xenopus skin: isolation, characterization of two active forms, and partial cDNA sequence of a precursor. *Proc. Natl. Acad. Sci. USA.* 84: 5449–5453.
22. Zasloff, M., B. Martin, and H. C. Chen. 1988. Antimicrobial activity of synthetic magainin peptides and several analogues. *Proc. Natl. Acad. Sci. USA.* 85:910–913.
23. Bechinger, B. 2005. Detergent-like properties of magainin antibiotic peptides: a ^{31}P solid-state NMR spectroscopy study. *Biochim. Biophys. Acta.* 1712:101–108.
24. Bechinger, B., M. Zasloff, and S. J. Opella. 1993. Structure and orientation of the antibiotic peptide magainin in membranes by solid-state nuclear magnetic resonance spectroscopy. *Protein Sci.* 2:2077–2084.
25. Duclohier, H., G. Molle, and G. Spach. 1989. Antimicrobial peptide magainin I from Xenopus skin forms anion-permeable channels in planar lipid bilayers. *Biophys. J.* 56:1017–1021.
26. Hallock, K. J., D. K. Lee, and A. Ramamoorthy. 2003. MSI-78, an analogue of the magainin antimicrobial peptides, disrupts lipid bilayer structure via positive curvature strain. *Biophys. J.* 84:3052–3060.
27. Jacob, L., and M. Zasloff. 1994. Potential therapeutic applications of magainins and other antimicrobial agents of animal origin. *Ciba Found. Symp.* 186:197–216.
28. Ramamoorthy, A., S. Thennarasu, D. K. Lee, A. Tan, and L. Maloy. 2006. Solid-state NMR investigation of the membrane-disrupting mechanism of antimicrobial peptides MSI-78 and MSI-594 derived from magainin 2 and melittin. *Biophys. J.* 91:206–216.
29. Ambroggio, E. E., F. Separovic, J. Bowie, and G. D. Fidelio. 2004. Surface behaviour and peptide-lipid interactions of the antibiotic peptides. Maculatin and citropin. *Biochim. Biophys. Acta.* 1664:31–37.
30. Ambroggio, E. E., F. Separovic, J. H. Bowie, G. D. Fidelio, and L. A. Bagatolli. 2005. Direct visualization of membrane leakage induced by the antibiotic peptides: maculatin, citropin, and aurein. *Biophys. J.* 89: 1874–1881.
31. Balla, M. S., J. H. Bowie, and F. Separovic. 2004. Solid-state NMR study of antimicrobial peptides from Australian frogs in phospholipid membranes. *Eur. Biophys. J.* 33:109–116.

32. Boland, M. P., and F. Separovic. 2006. Membrane interactions of antimicrobial peptides from Australian tree frogs. *Biochim. Biophys. Acta.* 1758:1178–1183.

33. Marcotte, I., K. L. Wegener, Y. H. Lam, B. C. Chia, M. R. de Planque, J. H. Bowie, M. Auger, and F. Separovic. 2003. Interaction of antimicrobial peptides from Australian amphibians with lipid membranes. *Chem. Phys. Lipids.* 122:107–120.

34. Niidome, T., K. Kobayashi, H. Arakawa, T. Hatakeyama, and H. Aoyagi. 2004. Structure-activity relationship of an antibacterial peptide, maculatin 1.1, from the skin glands of the tree frog, Litoria genimaculata. *J. Pept. Sci.* 10:414–422.

35. Chen, T., L. Li, M. Zhou, P. Rao, B. Walker, and C. Shaw. 2006. Amphibian skin peptides and their corresponding cDNAs from single lyophilized secretion samples: identification of novel brevinins from three species of Chinese frogs. *Peptides.* 27:42–48.

36. Conlon, J. M., N. Al-Ghaferi, B. Abraham, H. Jiansheng, P. Cosette, J. Leprince, T. Jouenne, and H. Vaudry. 2006. Antimicrobial peptides from diverse families isolated from the skin of the Asian frog, Rana grahami. *Peptides.* 27:2111–2117.

37. Kumari, V. K., and R. Nagaraj. 2001. Structure-function studies on the amphibian peptide brevinin 1E: translocating the cationic segment from the C-terminal end to a central position favors selective antibacterial activity. *J. Pept. Res.* 58:433–441.

38. Morikawa, N., K. Hagiwara, and T. Nakajima. 1992. Brevinin-1 and -2, unique antimicrobial peptides from the skin of the frog, Rana brevipoda porsa. *Biochem. Biophys. Res. Commun.* 189:184–190.

39. Simmaco, M., G. Mignogna, D. Barra, and F. Bossa. 1993. Novel antimicrobial peptides from skin secretion of the European frog Rana esculenta. *FEBS Lett.* 324:159–161.

40. Won, H. S., S. S. Kim, S. J. Jung, W. S. Son, B. Lee, and B. J. Lee. 2004. Structure-activity relationships of antimicrobial peptides from the skin of Rana esculenta inhabiting in Korea. *Mol. Cells.* 17:469–476.

41. Rozek, T., K. L. Wegener, J. H. Bowie, I. N. Olver, J. A. Carver, J. C. Wallace, and M. J. Tyler. 2000. The antibiotic and anticancer active aurein peptides from the Australian bell frogs Litoria aurea and Litoria raniformis the solution structure of aurein 1.2. *Eur. J. Biochem.* 267: 5330–5341.

42. Li, X., Y. Li, A. Peterkofsky, and G. Wang. 2006. NMR studies of aurein 1.2 analogs. *Biochim. Biophys. Acta.* 1758:1203–1214.

43. Rozek, T., J. H. Bowie, J. C. Wallace, and M. J. Tyler. 2000. The antibiotic and anticancer active aurein peptides from the Australian bell frogs Litoria aurea and Litoria raniformis. Part 2. Sequence determination using electrospray mass spectrometry. *Rapid Commun. Mass Spectrom.* 14:2002–2011.

44. Apponyi, M. A., T. L. Pukala, C. S. Brinkworth, V. M. Maselli, J. H. Bowie, M. J. Tyler, G. W. Booker, J. C. Wallace, J. A. Carver, F. Separovic, and others. 2004. Host-defence peptides of Australian anurans: structure, mechanism of action and evolutionary significance. *Peptides.* 25:1035–1054.

45. Wang, G., Y. Li, and X. Li. 2005. Correlation of three-dimensional structures with the antibacterial activity of a group of peptides designed based on a nontoxic bacterial membrane anchor. *J. Biol. Chem.* 280: 5803–5811.

46. Marion, D., and K. Wuthrich. 1983. Application of phase sensitive two-dimensional correlated spectroscopy (COSY) for measurements of ^{1}H-^{1}H spin-spin coupling constants in proteins. *Biochem. Biophys. Res. Commun.* 113:967–974.

47. Hwang, T. L., and A. J. Shaka. 1995. Water suppression that works: excitation sculpting using arbitrary wave-forms and pulsed-field gradients. *J. Magn. Reson. Ser. A.* 112:275–279.

48. Sinha, N., C. V. Grant, C. H. Wu, A. A. De Angelis, S. C. Howell, and S. J. Opella. 2005. SPINAL modulated decoupling in high field double- and triple-resonance solid-state NMR experiments on stationary samples. *J. Magn. Reson.* 177:197–202.

49. Wu, M., and R. E. Hancock. 1999. Interaction of the cyclic antimicrobial cationic peptide bactenecin with the outer and cytoplasmic membrane. *J. Biol. Chem.* 274:29–35.

50. Perham, M., J. Liao, and P. Wittung-Stafshede. 2006. Differential effects of alcohols on conformational switchovers in alpha-helical and beta-sheet protein models. *Biochemistry.* 45:7740–7749.

51. Wishart, D. S., C. G. Bigam, A. Holm, R. S. Hodges, and B. D. Sykes. 1995. ^{1}H, ^{13}C and ^{15}N random coil NMR chemical shifts of the common amino acids. I. Investigations of nearest-neighbor effects. *J. Biomol. NMR.* 5:67–81.

52. Chen, F. Y., M. T. Lee, and H. W. Huang. 2002. Sigmoidal concentration dependence of antimicrobial peptide activities: a case study on alamethicin. *Biophys. J.* 82:908–914.

53. Wu, Y., H. W. Huang, and G. A. Olah. 1990. Method of oriented circular dichroism. *Biophys. J.* 57:797–806.

54. de Jongh, H. H., E. Goormaghtigh, and J. A. Killian. 1994. Analysis of circular dichroism spectra of oriented protein-lipid complexes: toward a general application. *Biochemistry.* 33:14521–14528.

55. Tremouilhac, P., E. Strandberg, P. Wadhwani, and A. S. Ulrich. 2006. Synergistic transmembrane alignment of the antimicrobial heterodimer PGLa/magainin 2. *J. Biol. Chem.* 281:32089–32094.

56. Kucerka, N., M. A. Kiselev, and P. Balgavy. 2004. Determination of bilayer thickness and lipid surface area in unilamellar dimyristoylphosphatidylcholine vesicles from small-angle neutron scattering curves: a comparison of evaluation methods. *Eur. Biophys. J.* 33:328–334.

57. Dathe, M., H. Nikolenko, J. Meyer, M. Beyermann, and M. Bienert. 2001. Optimization of the antimicrobial activity of magainin peptides by modification of charge. *FEBS Lett.* 501:146–150.

58. Hallock, K. J., D. K. Lee, J. Omnaas, H. I. Mosberg, and A. Ramamoorthy. 2002. Membrane composition determines pardaxin's mechanism of lipid bilayer disruption. *Biophys. J.* 83:1004–1013.

59. Mani, R., J. J. Buffy, A. J. Waring, R. I. Lehrer, and M. Hong. 2004. Solid-state NMR investigation of the selective disruption of lipid membranes by protegrin-1. *Biochemistry.* 43:13839–13848.

60. Henzler Wildman, K. A., D. K. Lee, and A. Ramamoorthy. 2003. Mechanism of lipid bilayer disruption by the human antimicrobial peptide, LL-37. *Biochemistry.* 42:6545–6558.

61. Dave, P. C., E. Billington, Y. L. Pan, and S. K. Straus. 2005. Interaction of alamethicin with ether-linked phospholipid bilayers: oriented circular dichroism, ^{31}P solid-state NMR, and differential scanning calorimetry studies. *Biophys. J.* 89:2434–2442.

62. Falla, T. J., and R. E. Hancock. 1997. Improved activity of a synthetic indolicidin analog. *Antimicrob. Agents Chemother.* 41:771–775.

63. Zasloff, M. 2002. Antimicrobial peptides in health and disease. *N. Engl. J. Med.* 347:1199–1200.

64. Porcelli, F., B. A. Buck-Koehntop, S. Thennarasu, A. Ramamoorthy, and G. Veglia. 2006. Structures of the dimeric and monomeric variants of magainin antimicrobial peptides (MSI-78 and MSI-594) in micelles and bilayers, determined by NMR spectroscopy. *Biochemistry.* 45: 5793–5799.

65. Wu, Y., K. He, S. J. Ludtke, and H. W. Huang. 1995. X-ray diffraction study of lipid bilayer membranes interacting with amphiphilic helical peptides: diphytanoyl phosphatidylcholine with alamethicin at low concentrations. *Biophys. J.* 68:2361–2369.

66. Harzer, U., and B. Bechinger. 2000. Alignment of lysine-anchored membrane peptides under conditions of hydrophobic mismatch: a CD, ^{15}N and ^{31}P solid-state NMR spectroscopy investigation. *Biochemistry.* 39:13106–13114.

67. Matsuzaki, K., O. Murase, N. Fujii, and K. Miyajima. 1996. An antimicrobial peptide, magainin 2, induced rapid flip-flop of phospholipids coupled with pore formation and peptide translocation. *Biochemistry.* 35:11361–11368.

68. Kyte, J., and R. F. Doolittle. 1982. A simple method for displaying the hydropathic character of a protein. *J. Mol. Biol.* 157:105–132.